JBC Papers in Press. Published on June 10, 2009 as Manuscript C109.016931
The latest version is at http://www.jbc.org/cgi/doi/10.1074/jbc.C109.016931

INHIBITION OF HUMAN STEROID 5β-REDUCTASE (AKR1D1) BY FINASTERIDE AND STRUCTURE OF THE ENZYME-INHIBITOR COMPLEX

Jason E. Drury[1], Luigi Di Costanzo[3], Trevor M. Penning[1,2], and David W. Christianson[3]
From Center of Excellence in Environmental Toxicology[2] and Department of Pharmacology[1], University of Pennsylvania School of Medicine, Philadelphia, Pennsylvania, 19104-6084; Roy and Diana Vagelos Laboratories[3], Department of Chemistry, University of Pennsylvania, Philadelphia, Pennsylvania, 19104-6323, United States

Running title: Steroid 5β-reductase finasteride complex

Address all correspondence to: Dr. Trevor M. Penning, Department of Pharmacology, University of Pennsylvania, 130C John Morgan Bldg., 3620 Hamilton Walk, Philadelphia, PA, 19104-6084. Phone: 215-898-9445; Fax: 215-573-2236; Email: penning@mail.med.upenn.edu; Dr. David W. Christianson, Roy and Diana Vagelos Laboratories, Department of Chemistry, University of Pennsylvania, Philadelphia, PA 19104-6323. Phone: 215-898-5714; Fax: 215-573-2201; Email: chris@sas.upenn.edu.

The Δ^4-3-ketosteroid functionality is present in nearly all steroid hormones apart from estrogens. The first step in functionalization of the A-ring is mediated in humans by steroid 5α- or 5β-reductase. Finasteride is a mechanism-based inactivator of 5α-reductase type 2 with sub-nanomolar affinity and is widely used as a therapeutic for the treatment of benign prostatic hyperplasia. It is also used for androgen deprivation in hormone dependent prostate carcinoma and it has been examined as a chemopreventive agent in prostate cancer. The effect of finasteride on steroid 5β-reductase (AKR1D1) has not been previously reported. We show that finasteride competitively inhibits AKR1D1 with low micromolar affinity but does not act as a mechanism-based inactivator. The structure of the AKR1D1·$NADP^+$·finasteride complex determined at 1.7 Å resolution shows that it is not possible for NADPH to reduce the Δ^{1-2}-ene of finasteride since the cofactor and steroid are not proximal to each other. The C3-ketone of finasteride accepts hydrogen bonds from the catalytic residues Y58 and E120 in the active site of AKR1D1, providing an explanation for the competitive inhibition observed. This is the first reported structure of finasteride bound to an enzyme involved in steroid hormone metabolism.

The Δ^4-3-ketosteroid functionality is present in many important steroid hormones, e.g., testosterone, cortisone, and progesterone. An initial step in steroid hormone metabolism is the reduction of the Δ^4-ene, which in humans is mediated by steroid 5α-reductases (SRD5A1, SRD5A2) or steroid 5β-reductase (AKR1D1) to yield the corresponding 5α- or 5β-dihydrosteroids, respectively (1,2). The products of these reactions are not always inactive. 5α-Reductase is responsible for the conversion of testosterone to 5α-dihydrotestosterone, which is the most potent natural ligand for the androgen receptor. By contrast, in addition to being involved in bile-acid biosynthesis, 5β-reductase is responsible for generating 5β-pregnanes which are natural ligands for the pregnane-X receptor (PXR) in the liver (3,4). PXR is involved in the induction of CYP3A4, which is responsible for the metabolism of a large proportion of drugs (5,6). Thus both 5α- and 5β-reductase are involved in the formation of potent ligands for nuclear receptors.

Finasteride is a selective 5α-reductase type 2 inhibitor which reduces plasma 5α-DHT levels and shrinks the size of the prostate (7). It is a widely used therapeutic agent in the treatment of benign prostatic hyperplasia (BPH) (8,9), it is used in androgen deprivation therapy to treat prostate cancer (10), and it has been examined as a chemopreventive agent for hormone dependent prostate cancer (11). Finasteride was originally thought to act as a competitive inhibitor with nanomolar affinity for 5α-reductase type 2 (12). More recently, it was found that finasteride acts as a mechanism-based inactivator of this enzyme (13). Subsequent to inhibitor binding there is hydride transfer from the NADPH cofactor to the $\Delta^{1,2}$-ene-double bond of finasteride. The intermediate enolate tautomerizes at the enzyme active site to form a bisubstrate analog in which dihydrofinasteride is covalently bound to $NADP^+$ (13). The bi-substrate analogue has sub-nanomolar

affinity for 5α-reductase type 2 (Fig. 1). No structural information exists for 5α-reductase type 1 or type 2; therefore, it is not possible to determine how finasteride would bind to the active site of a human steroid-double bond reductase in the absence of an experimentally determined crystal structure.

Human steroid 5β-reductase is a member of the aldo-keto reductase (AKR) superfamily and is formally designated (AKR1D1) (14). The AKRs are soluble NADP(H)-dependent oxidoreductases with monomeric molecular weights of 37 kDa. These enzymes are amenable to X-ray crystallography and during the last year we and others have reported crystal structures of ternary complexes of AKR1D1 (15-17). The ternary complexes containing steroid substrates include: AKR1D1·$NADP^+$·testosterone (PDB: 3BUR), AKR1D1·$NADP^+$·progesterone (PDB: 3COT), AKR1D1·$NADP^+$·cortisone (PDB: 3CMF), and AKR1D1·$NADP^+$·Δ^4-androstene-3,17-dione (PDB: 3CAS) (17). In addition, ternary complexes containing the products 5β-dihydroprogesterone (PDB: 3CAV) and 5β-dihydrotestosterone (PDB: 3DOP) have also been described (16,18).

As part of an ongoing inhibitor screen of AKR1D1, we now report that finasteride acts as a competitive inhibitor with low micromolar affinity. Additionally, we report the X-ray crystal structure of the AKR1D1·$NADP^+$·finasteride complex.

EXPERIMENTAL PROCEDURES

Materials–The pET16b and pET28a vectors were purchased from Novagen. The *E. coli* strain C41 (DE3) was provided by Dr. J. E. Walker (MRC Laboratory of Molecular Biology, Cambridge, U.K.). NADPH was obtained from Roche. Steroids were purchased from Steraloids, Inc. [4-^{14}C]-Testosterone (50 mCi/mmol) was obtained from PerkinElmer Life and Analytical Sciences. Finasteride was obtained from Merck Research Laboratories. All other reagents were of ACS quality or higher.

Expression of Recombinant AKR1D1–Previously we reported the expression of AKR1D1 using the prokaryotic expression vectors pET16b and pET28a (15). Recombinant AKR1D1 was purified to homogeneity as described previously (15). Wild-type AKR1D1 was obtained in 56% yield and had a final specific activity of 80 nmoles of testosterone reduced per minute per mg of purified enzyme under standard radiometric assay conditions.

Standard Radiometric Assay and Product Verification–The standard assay contained 2 μM [4-^{14}C] testosterone (40,000 dpm), 8 μM unlabeled testosterone, 5% acetonitrile, and 100 mM phosphate buffer (pH 6.0). Reactions were initiated by the addition of 200 μM NADPH and performed at 37 °C. The substrate and product of the quenched reaction were separated by TLC and quantitated by scintillation counting. The 5β-dihydrotestosterone (5β-DHT) product was identified by co-chromatography with the authentic standard.

Standard Spectrofluorimetric Assay–Spectrofluorimetric analysis of the reduction of testosterone to 5β-DHT was performed by monitoring the decrease in NADPH emission on a fluorescence spectrophotometer F-4500 (Hitachi America, Ltd., New York, NY). Assays contained 10 μM testosterone, 15 μM NADPH, 4% acetonitrile in 100 mM potassium phosphate buffer (pH 6.0) in a final volume of 1 mL. Reactions were initiated by the addition of enzyme and monitored at 37 °C. NADPH emission was monitored by using an excitation wavelength of 340 nm (slit-width 5 nm) and an emission wavelength set at 460 nm (slit-width 10 nm). A standard curve was performed daily, to convert the arbitrary fluorescence units measured at 460 nm to NADPH concentration. The curve was used to calculate the amount of NADPH oxidized per minute in the assays. The specific activity observed was in agreement with the specific activity measured radiometrically and gave a value of 80 nmoles of testosterone reduced per minute per mg of purified enzyme.

Enzyme Inhibition Studies–Enzyme inhibition studies were performed using the standard radiometric assay to monitor the reduction of 2.0 μM [^{14}C]-testosterone in the absence or presence of increasing finasteride concentrations at 37 °C. The K_i value was determined by producing a family of lines using different fixed substrate concentrations and by varying the finasteride concentration. The family of lines was fit using GraFit and the pattern was examined to determine the mode of inhibition, i.e.,

competitive, noncompetitive and uncompetitive. Time-dependent incubation studies were performed with finasteride in which AKR1D1 (7.8 μM) was preincubated with finasteride (31.0 μM) in the presence and absence of NADPH (144 μM) in 100 mM buffer (pH 6.0) at 37 °C. Aliquots were removed from the incubation over time and directly diluted (100-fold dilution) into the standard spectrofluorimetric assay and the amount of enzyme activity remaining was determined.

Crystallography–The AKR1D1·$NADP^+$·finasteride complex was crystallized by the hanging drop vapor diffusion method at 4 °C. Typically, a drop containing 3.0 μL of enzyme solution [5.0 mg/mL AKR1D1, 2.0 mM $NADP^+$, 0.5 mM finasteride, 10.0 mM Tris (pH 7.4)] and 4.0 μL of precipitant buffer [0.1 M Tris-HCl (pH 7.0), 10-20% (wt/vol) PEG 4000, 10% isopropanol] was equilibrated against a 1 mL reservoir of precipitant buffer. Crystals of the AKR1D1·$NADP^+$·finasteride complex appeared within one week and were then soaked for 24 h in the same mother liquor solution augmented with 2.0 mM $NADP^+$, 2.0 mM finasteride and 30% isopropanol. Following transfer to a 32% Jeffamine solution and flash-cooling, these crystals yielded diffraction data to 1.70 Å resolution at the National Synchrotron Light Source (beamline X6A, λ=1.00 Å, 100 K). Diffraction intensities measured from these crystals indicated that they belonged to the space group $P2_12_12_1$ with unit cell parameters similar to those previously measured from crystals of AKR1D1 complexed with different steroids (15). Two monomers occupy the asymmetric unit in this crystal form. Data reduction was achieved using the programs HKL2000 and SCALEPACK (19). Data collection and reduction statistics are reported in Table 1.

The structure of the AKR1D1·$NADP^+$·finasteride complex was solved by the difference Fourier method using the model of the AKR1D1·$NADP^+$·cortisone complex less ligand atoms and water molecules (PDB: 3CMF) as a starting model. The programs CNS (20) and PHENIX.refine (21) were used to refine the model and the graphics program Coot (22) was used for map fitting. In the final stage of refinement, the atomic coordinates of finasteride were retrieved from entry WOLXEA (23) in the Cambridge Structural Database (24) and built into the electron density map. Data collection and refinement statistics are reported in Table 1.

RESULTS

Inhibition Studies–Finasteride, which is a mechanism-based inhibitor of 5α-reductase with sub-nanomolar affinity, is a competitive inhibitor of recombinant AKR1D1 with a K_i value of 2.1 μM when AKR1D1 is saturated with NADPH and testosterone is used as a varied substrate (Fig. 2). Knowing that finasteride is a mechanism-based inactivator of 5α-reductase type 2 and that the mechanism of inactivation has an obligatory requirement for NADPH, we conducted preincubation studies of AKR1D1 with finasteride in the presence and absence of added NADPH over 140 mins. Upon dilution of aliquots into a standard AKR1D1 activity assay, we obtained no evidence for time-dependent inactivation of the enzyme.

Structure of the AKR1D1·$NADP^+$·Finasteride Complex–Finasteride is bound with full occupancy to monomer B in the crystal structure of the AKR1D1·$NADP^+$·finasteride complex. The structure of this complex is very similar to the crystal structures of the ternary AKR1D1 complexes containing $NADP^+$ and either cortisone or progesterone, with root-mean-square (r.m.s.) deviations of ~0.20 Å for 324 Cα atoms (15). The electron density envelope of finasteride is clear and unambiguous (Fig. 3a), showing that the steroid binds perpendicular to the $NADP^+$ cofactor.

The side chain of W230 plays a key role in packing against the β-face of finasteride, which is oriented towards the *re*-face of the nicotinamide ring of $NADP^+$ such that the steroid C1-C2 double bond is too far away from the 4-pro-*R*-hydride of NADPH for double-bond reduction to occur (Fig. 3a). The C3 carbonyl oxygen of finasteride accepts hydrogen bonds from the phenolic hydroxyl group of Y58 and the *anti*-oriented conformer of the carboxylic acid side chain of E120. Additionally, the N4 group and the C20 carbonyl oxygen group of finasteride engage in hydrogen bond interactions with water molecules (Fig. 3a). Interestingly, even though the binding mode of finasteride is similar to that of progesterone, finasteride is rotated by ~12° with respect to

progesterone (Fig. 3b), and the segment R226-V231 (which contains W230) in loop B moves ~1 Å away to accommodate finasteride binding in comparison with progesterone binding.

In monomer A, continuous but uninterpretable electron density is observed, possibly indicating disordered or low occupancy binding of finasteride (Fig. S1, Supporting Information). Accordingly, we have not built finasteride into this density in the final model. Finally, in both monomers the backbone conformation of T224 adopts a disallowed conformation on the Ramachandran plot. Notably, the electron density corresponding to T224 is clear and continuous (data not shown). Since T224 is adjacent to the substrate and cofactor binding sites (15), it is possible that its unfavorable backbone conformation is accommodated to optimize enzyme function. Herzberg and Moult (25) observe that regions of such steric strain in refined enzyme structures are located overwhelmingly in or near active sites, concluding that the precision required for substrate binding and catalysis occasionally outweighs the requirement for optimal protein folding.

Reduction of $\Delta^{1,4}$-Dienes. To validate that AKR1D1 is unable to reduce a $\Delta^{1,2}$-ene double bond, 1,4-androstadien-17β-ol-3-one was examined as a substrate; co-chromatography with authentic standards was used to identify the product of the reaction. The reaction has three possible product outcomes: testosterone from reduction of the $\Delta^{1\text{-}2}$-ene; 5β-androst-1-en-17β-ol-3-one from reduction of the $\Delta^{4\text{-}5}$-ene; or 5β-DHT from reduction of the $\Delta\text{-}^{1,4}$-diene. The product does not co-migrate with either testosterone or 5β-DHT, suggesting that the enzyme is unable to reduce the $\Delta^{1\text{-}2}$-ene. The k_{cat} and K_m for this reaction are 1.8 min^{-1} and 3.2 μM, respectively.

DISCUSSION

AKR1D1 is inhibited by the 5α-reductase type 2 selective inhibitor finasteride, by acting solely as a reversible competitive inhibitor. The K_i value of 2.1 μM is considerably higher than that observed for either the competitive inhibition or time-dependent inactivation of 5α-reductase type 2. By contrast, the K_i value of 2.1 μM is less than an order of magnitude greater than that observed for the inhibition of 5α-reductase type 1 (K_i value of 300 nM) (26). Both AKR1D1 and 5α-reductase type 1 play important roles in the hepatic clearance of steroid hormones, suggesting that high-dose finasteride may have an adverse effect on hepatic steroid metabolism. Inhibition of AKR1D1 by high-dose finasteride would also deprive PXR of its natural 5β-pregnane ligands, resulting in diminished CYP3A4 induction. This could result in significant drug-drug interactions. Importantly, finasteride itself is metabolized by CYP3A4, suggesting that high-dose finasteride might prevent its own metabolism (27).

Finasteride does not act as a mechanism-based inactivator of AKR1D1, in contrast with its mode of inhibition against 5α-reductase type 2. Although both AKR1D1 and 5α-reductase type 2 reduce the 4-5 double bond of Δ^4-3-oxosteroids in a similar manner, i.e., hydride transfer to C5 followed by enolization, the structure of the AKR1D1·$NADP^+$·finasteride complex (Fig. 2a) shows that it is not possible to reduce the $\Delta^{1\text{-}2}$-ene of finasteride because this double bond is not proximal to the NADPH cofactor. The similarity in the binding orientations of finasteride and progesterone to AKR1D1, however, account for the competitive inhibition of 5β-reductase by the drug. It is noteworthy that finasteride forms hydrogen bonds with Y58 and E120 which are part of the catalytic tetrad of AKR1D1.The inability to reduce a $\Delta^{1\text{-}2}$-ene is validated by using 1,4-androstadien-17β-ol-3-one as a substrate.

No structural information currently exists for 5α-reductase type 2. However, based on the structure of the AKR1D1·$NADP^+$·finasteride complex, it is anticipated that the cofactor must be aligned for $\Delta^{1\text{-}2}$-ene reduction. It will also be intriguing to see whether there is conservation in catalytic mechanism. We have previously proposed with the aid of site-directed mutagenesis that double bond reduction requires both a catalytic tyrosine (Y58) and a superacidic glutamic acid residue (E120) (15,18). Future X-ray crystallographic studies will determine whether such a mechanism operates for 5α-reductase type 1 and type 2.

REFERENCES

1. Russell, D. W. (2003) *Annu. Rev. Biochem.* 72, 137-174
2. Russell, D. W., and Wilson, J. D. (1994) *Annu. Rev. Biochem.* 63, 25-61
3. Bertilsson, G., Heidrich, J., Svensson, K., Asman, M., Jendeberg, L., Sydow-Backman, M., Ohlsson, R., Postlind, H., Blomquist, P., and Berkenstam, A. (1998) *Proc. Natl. Acad. Sci. U. S. A.* 95, 12208-12213
4. Moore, L. B., Parks, D. J., Jones, S. A., Bledsoe, R. K., Consler, T. G., Stimmel, J. B., Goodwin, B., Liddle, C., Blanchard, S. G., Willson, T. M., Collins, J. L., and Kliewer, S. A. (2000) *J. Biol. Chem.* 275, 15122-15127
5. Huang, W., Ma, K., Zhang, J., Qatanani, M., Cuvillier, J., Liu, J., Dong, B., Huang, X., and Moore, D. D. (2006) *Science* 312, 233-236
6. Shimada, T., Yamazaki, H., Mimura, M., Wakamiya, N., Ueng, Y. F., Guengerich, F. P., and Inui, Y. (1996) *Drug Metab. Dispos.* 24, 515-522
7. Stoner, E. (1990) *J. Steroid Biochem. Mol. Biol.* 37, 375-378
8. Gormley, G. J. (1996) *Semin. Urol. Oncol.* 14, 139-144
9. Habib, F. K., Ross, M., Tate, R., and Chisholm, G. D. (1997) *Clin. Endocrinol. (Oxf)* 46, 137-144
10. Andriole, G., Lieber, M., Smith, J., Soloway, M., Schroeder, F., Kadmon, D., DeKernion, J., Rajfer, J., Boake, R., Crawford, D., and et al. (1995) *Urology* 45, 491-497
11. Thompson, I. M., Goodman, P. J., Tangen, C. M., Lucia, M. S., Miller, G. J., Ford, L. G., Lieber, M. M., Cespedes, R. D., Atkins, J. N., Lippman, S. M., Carlin, S. M., Ryan, A., Szczepanek, C. M., Crowley, J. J., and Coltman, C. A., Jr. (2003) *N. Engl. J. Med.* 349, 215-224
12. Andersson, S., and Russell, D. W. (1990) *Proc. Natl. Acad. Sci. U. S. A.* 87, 3640-3644
13. Bull, H. G., Garcia-Calvo, M., Andersson, S., Baginsky, W. F., Chan, H. K., Ellsworth, D. E., Miller, R. R., Stearns, R. A., Bakshi, R. K., Rasmusson, G. H., Tolman, R. L., Myers, R. W., Kozarich, J. W., and Harris, G. S. (1996) *J. Am. Chem. Soc.* 118, 2359-2365
14. Jez, J. M., Bennett, M. J., Schlegel, B. P., Lewis, M., and Penning, T. M. (1997) *Biochem. J.* 326 (Pt 3), 625-636
15. Di Costanzo, L., Drury, J. E., Penning, T. M., and Christianson, D. W. (2008) *J. Biol. Chem.* 283, 16830-16839
16. Faucher, F., Cantin, L., Luu-The, V., Labrie, F., and Breton, R. (2008) *Biochemistry* 47, 8261-8270
17. Faucher, F., Cantin, L., Luu-The, V., Labrie, F., and Breton, R. (2008) *Biochemistry* 47, 13537-13546
18. Di Costanzo, L., Drury, J. E., Christianson, D. W., and Penning, T. M. (2009) *Mol. Cell. Endocrinol.* 301, 191-198
19. Otwinowski, Z., Minor, W., and Charles W. Carter, Jr. (1997) Processing of X-ray diffraction data collected in oscillation mode. in *Methods in Enzymology*, Academic Press. pp 307-326
20. Brünger, A. T., Adams, P. D., Clore, G. M., DeLano, W. L., Gros, P., Grosse-Kunstleve, R. W., Jiang, J. S., Kuszewski, J., Nilges, M., Pannu, N. S., Read, R. J., Rice, L. M., Simonson, T., and Warren, G. L. (1998) *Acta Crystallogr. Sect. D Biol. Crystallogr.* 54, 905-921
21. Afonine, P. V., Grosse-Kunstleve, R. W., and Adams, P. D. (2005) *Acta Crystallogr. Sect. D Biol. Crystallogr.* 61, 850-855
22. Emsley, P., and Cowtan, K. (2004) *Acta Crystallogr. Sect. D Biol. Crystallogr.* 60, 2126-2132
23. Wawrzycka, I., Stepniak, K., Matyjaszczyk, S., Koziol, A. E., Lis, T., and Abboud, K. A. (1999) *J. Mol. Struct.* 474, 157-166
24. Allen, F. H. (2002) *Acta Crystallogr. Sect. D Biol. Crystallogr.* 58, 380-388

25. **Herzberg, O., and Moult, J. (1991)** ***Proteins*** **11, 223-229**
26. **Jenkins, E. P., Andersson, S., Imperato-McGinley, J., Wilson, J. D., and Russell, D. W. (1992)** ***J. Clin. Invest.*** **89, 293-300**
27. **Huskey, S. W., Dean, D. C., Miller, R. R., Rasmusson, G. H., and Chiu, S. H. (1995)** ***Drug Metab. Dispos.*** **23, 1126-1135**

FOOTNOTES

*This work was supported by National Institutes of Health Grants R01-DK47015 and P30-ES013508 awarded to T.M.P. and R01-GM56838 awarded to D.W.C.

The abbreviations used are: AKR, aldo-keto reductase; AKR1D1, human liver 5β-reductase; 5α-DHT, 5α-dihydrotestosterone; PXR, pregnane-X receptor; r.m.s., root-mean-square.

The atomic coordinates and structure factors of the AKR1D1-NADP$^+$-finasteride complex have been deposited in the Protein Data Bank (www.rcsb.org) with accession code 3G1R.

FIGURE LEGENDS

FIGURE 1. **Mechanism-Based Inactivation of 5α-Reductase Type 2 by Finasteride.** Adapted from Bull et al. (13). R = -C(=O)-NH_2

FIGURE 2. **Competitive Inhibition of AKR1D1 by Finasteride.** Lineweaver–Burke plots demonstrate that finasteride exhibits a competitive inhibition pattern for the reduction of testosterone catalyzed by AKR1D1. Assays were performed as described in the Materials and Methods section.

FIGURE 3. **AKR1D1·NADP$^+$·finasteride complex.** *Panel A*, Stereoview of simulated annealing omit electron density map of the AKR1D1·NADP$^+$·finasteride complex contoured at 3.0σ. Atoms are color coded as follows: C = green, N = blue, O = red, P = orange; water molecules appear as red spheres. Finasteride hydrogen bond interactions are indicated by dashed green lines. *Panel B*, Least-squares superposition of Cα atoms of the AKR1D1·NADP$^+$·finasteride complex (color coded as in (a)) and the AKR1D1·NADP$^+$·progesterone complex (3COT, (15)) (all atoms are magenta). The indole ring of W230 and the segment R226-V231 of its associated loop B moves ~1 Å away to accommodate the binding of finasteride compared with the binding of progesterone.

Table 1. Data Collection and Refinement Statistics for the AKR1D1·$NADP^+$·Finasteride Complex

Data collection	
Resolution range (Å)	30.0–1.70
Unique reflections measured	76,941 (7,211)
R_{merge} [a]	0.049 (0.35)[b]
I/σ(I)	25.3 (3.5)[b]
Completeness (%)	97.8 (92.9)[b]
Refinement statistics	
Reflections used in refinement/test set	73,561/3,717
R/R_{free} [c]	0.174/0.205
Protein atoms[d]	5,254
Water molecules[d]	754
$NADP^+$ molecules[d]	2
Finasteride molecules[d,e]	1
Average B factors (Å^2)	
Protein main chain atoms	15
Protein side chain atoms	19
Water molecules	26
Finasteride	29
NADP	19
Ramachandran plot	
Most favored region (%)	89.0
Additionally allowed region (%)	10.7
Generously allowed region (%)	0.2
Disallowed region (%)	0.2
MolProbity	
Clashscore, all atoms/percentile	6.8/88
Rotamer outliers (%)	1.2
Ramachandran outliers (%)	0.0
Ramachandran favored (%)	97.7
MolProbity score/percentile	1.5/91
Residues with bad bonds (%)	0.0
Residues with bad angles (%)	0.0
Cβ deviations >0.25 Å	0
R.m.s. deviations	
Bond lengths (Å)	0.006
Bond angles (deg)	1.00
Dihedral angles (deg)	16.9

[a] $R_{merge} = \sum| I - \langle I \rangle | / \sum I$, where I is the observed intensity and $\langle I \rangle$ is the average intensity calculated for replicate data.
[b] The number in parentheses refer to the outer 0.1-Å shell of data.
[c] Crystallographic R-factor, $R = \sum(| F_o | - | F_c |)/\sum | F_o |$, for reflections contained in the working set. The same expression is used to calculate R_{free} using reflections contained in the test set excluded from refinement. $| F_o |$ and $| F_c |$ are the observed and calculated structure factor amplitudes, respectively.
[d] Per asymmetric unit.
[e] Monomer B only.

Figure 1

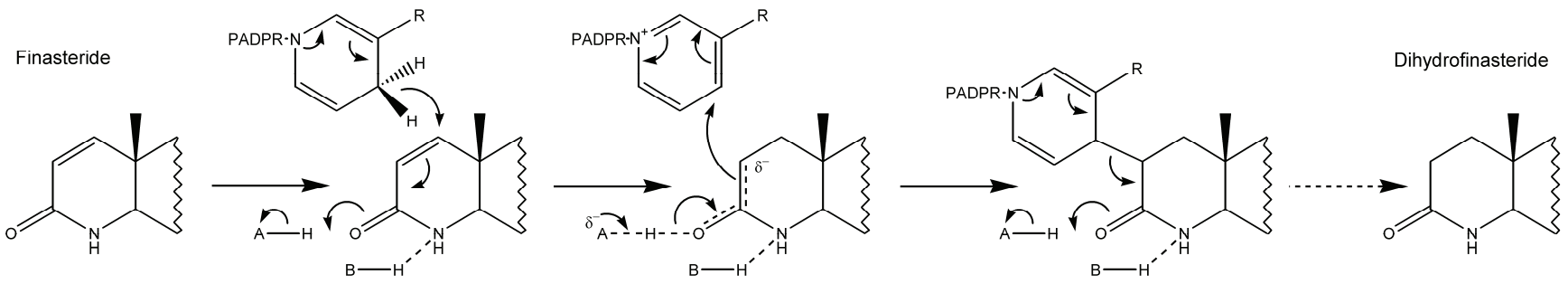

Figure 2

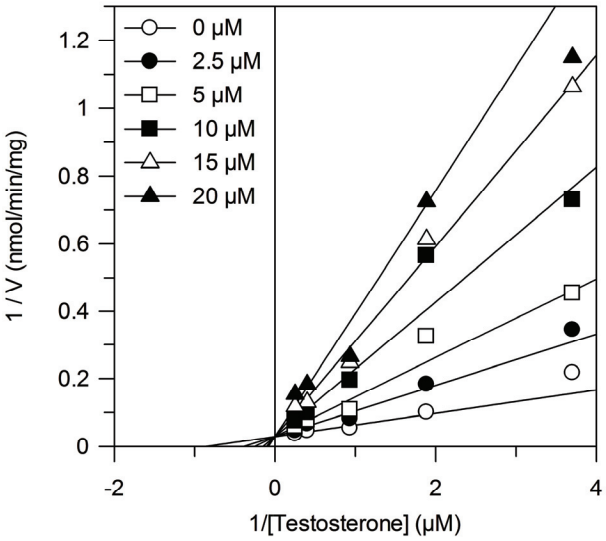

Figure 3